OKU Fen Bilimleri Enstitüsü Dergisi
8(1): 167-181, 2025

OKU Journal of The Institute of Science and Technology, 8(1): 167-181, 2025

Osmaniye Korkut Ata Üniversitesi
Fen Bilimleri Enstitüsü
Dergisi

Osmaniye Korkut Ata University
Journal of The Institute of Science
and Technology

An Investigation of Four-Point Bending Behavior for Personalized Humerus Bone Plate

Hakan Burçin ERDOĞUŞ[1*]

[1]Izmır Kavram Vocational School, Machinery and Metal Technologies Department, Machinery Programme, Izmir, Türkiye

[1]https://orcid.org/0000-0002-2947-7510
*Corresponding author:hakan.erdogus@kavram.edu.tr

Research Article

Article History:
Received: 29.04.2024
Accepted: 23.08.2024
Published online: 15.01.2025

Keywords:
Bone plates
Method of anatomical features
Four-point bending tests
Personalized bone plate

ABSTRACT

The reverse engineering method has been beneficial for personalized implant designs in the medical field due to its flexible use feature that allows it to be applied in many areas. The method of anatomical features (MAF) is commonly used for fractures of the bone for the development of plate fixation. To improve the geometrical fitting between plate and bone, high-quality image data is the most important factor for computer aided design (CAD) modelling. This study aims to use MAF for humerus bone plate design that would alternate the fracture region and decrease the stress-shielding effect depending on bending strength. For this purpose, the personalized plate implant (PPI) was designed according to MAF and fabricated using the multi jet fusion (MJF) technique, finally the four-point bending finite element analysis was applied and tested. The results indicated that the PPI structure has higher bending strength than the flat plate design and a much greater surface area.

Kişiselleştirilmiş Humerus Kemik Plakasının Dört Noktalı Eğilme Davranışının İncelenmesi

Araştırma Makalesi

Makale Tarihçesi:
Geliş tarihi: 29.04.2024
Kabul tarihi: 23.08.2024
Online Yayınlanma: 15.01.2025

Anahtar Kelimeler:
Kemik plakaları
Anatomik özellikler yöntemi
Dört nokta eğilme testleri
Kişiselleştirilmiş kemik plakası

ÖZ

Tersine mühendislik yöntemi birçok alanda uygulanmasına olanak sağlayan esnek kullanım özelliği nedeniyle tıp alanında kişiye özel implant tasarımlarında fayda sağlamıştır. Anatomik özellikler yöntemi (MAF), plak fiksasyonunun geliştirilmesi için kemik kırıklarında yaygın olarak kullanılmaktadır. Plaka ve kemik arasındaki geometrik uyumu iyileştirmek için yüksek kaliteli görüntü verileri CAD modellemede en önemli faktördür. Bu çalışma; kırık bölgesini değiştirecek ve bükülme mukavemetine bağlı olarak stres koruyucu etkiyi azaltacak humerus kemik plakası tasarımı için MAF'ın kullanılmasını amaçlamaktadır. Bu amaçla kişiselleştirilmiş plaka implant (PPI), MAF'a göre tasarlanıp, multi jet füzyon (MJF) tekniği kullanılarak üretilmiştir. Son olarak dört nokta bükme sonlu elemanlar analizi uygulanarak test edilmiştir. Sonuçlar, PPI yapısının düz plaka tasarımına göre daha yüksek bükülme mukavemetine ve çok daha büyük bir yüzey alanına sahip olduğunu göstermiştir.

To Cite: Erdoğuş HB. An Investigation of Four-Point Bending Behavior for Personalized Humerus Bone Plate. Osmaniye Korkut Ata Üniversitesi Fen Bilimleri Enstitüsü Dergisi 2025; 8(1): 167-181.

1. Introduction

In recent years, three-dimensional (3D) models produced by additive manufacturing (AM) methods have been used in patient-specific implant and prosthesis designs. To creating a 3D physical model begins with processing computer tomography (CT) and magnetic resonance imaging (MRI) digital data with appropriate methods. These images are used in pre-clinical evaluations to discuss the procedure and make the most appropriate decision (Huatilainen et al., 2014; Malik et al., 2015; Marro et al., 2016). Arvier et al., (1994) concluded that maxillofacial 3D models are useful in visualizing the dimensional movement of bones for preoperative adaptation at the surgical planning stage. In addition, these models with similar accuracy provide efficiency in terms of cost by reducing post-operative complications, early-term diagnosis, and decreased operation time (Webb, 2000; Cousley et al., 2017). It becomes important to create an anatomical model by obtaining high-quality image data from the maxillofacial region. Cone beam computer tomography (CBCT) is among the slicing techniques used in creating 3D biomodels, assets in implant planning, predicting maxillofacial growth, and determining bone volume in the reconstruction process for orthodontic surgery (Liang et al., 2010a; Liang et al., 2010b).

Method of anatomical features (MAF) is frequently used in modeling and reverse engineering of human bones. The main purpose of the MAF method is to gain close anatomical structure by developing a bone 3D model with highly geometric precision. In the study that investigated based on the femur and tibia bones model, it was stated that the accuracy between the polygonal model and bone geometric morphology was adequate for plate design. Additionally, it has been concluded that a 3D geometric model can be created even in cases where there is partial data about human bone (Majstonovic et al., 2013; Vitković et al., 2019). Shoulkha et al., (2011) created a 3D model with the help of geometrically simulated shapes (ellipsoid and hyperbolic) similar to the anatomical landmarks on the femoral bone surface. A mean fitting error of 0.5-1.2 mm occurred between this 3D model and image data. In a similar study, according to geometric measurements, there was a deviation of less than 1 mm in 75% of the entire geometry between the 3D model prepared with the MAF method and the input data (Rashid, 2023).

The fixation plates are commonly used in the treatment of fractures in the distal-proximal or shaft of human bones as a result of injury. The personalized plate implant (PPI) designed for the repair of distal femur fractures aims to ensure continuity in blood flow by matching the deformed surfaces to each other after deformation. Chen, (2018) examined the stress distribution on the personalized fixation plate according to the surface geometry created by restoring the broken femur bone. For complex geometries such as bone structure, feature-based definition reduces the time for editing and ensures optimal plate design. To overcome stress shielding of femoral shaft fracture and enhanced wrap of bone-plate couple, stress and deformation are significantly reduced by preparing a customized plate design (Soni and Sing, 2020). To improve the PPI for tibial bone fracture, stress distribution, and stress shielding rate are reduced with the groove design on the plate (Liao et al., 2021). However, loss of movement function and pain that occurs after the healing process of tibial plateau fractures restricts the activities of patients. Due to the posterolateral region being complex, the plate should be placed on the bone contour to wrap the fracture fragments correctly. To perform the process such as bending the flat plates to settle in the plateau region causes longer surgery time, increases blood loss, and weakness the mechanical properties of the plate (Jian et al., 2018; Ren et al., 2018). Proximal humerus, humeral shaft, and distal humerus fractures are frequently observed in adult and elderly people. Meanwhile, due to fractures of the proximal humerus and displacement of fragments, satisfactory results were not obtained in the treatment with traditional plates and screws (Kumar et al., 2013; Nowak et al., 2018). The compatibility of the screw and the plate used as screws should be sufficient for the fracture region to be covered by the plate. In this case, the increase in the distance between the bone and the plate in the application of an extraperiosteal locking plate has a significant impact on the stability of the construction (Ahmed et al., 2007). As a result of parametric optimization for the proximal humerus plate, Jabran et al., (2019) determined that the plate bending strength depends on the screws close to the proximal region. Tilton et al., (2020) emphasized the importance of medial support with plate fixation applied to proximal humerus fractures. Moreover, it has been found that new medial support leads to a significant reduction in humeral head migration under increasing repetitive loads. The plates used in extra-articular humerus fractures provide stability in terms of fixation and resistance to torsion forces (Scalaro et al., 2014). It has been reported that mid-distal humeral shaft fractures can be successfully treated with a minimally invasive plate (MIPA). Moreover, with this technique, there is less soft tissue dissection which eliminates the need to expose the radial nerve (An et al., 2010). The main benefit of the MAF technique is the use of personalized specific features. By applying the parametric design method of the fixing plate, a structure compatible with the humeral shaft topology is prepared (Rashid et al., 2017; Rashid et al., 2021).

In this study, MAF was applied for left humeral shaft bone fracture. For this purpose, input data transferred from medical imaging techniques was used at the base of the investigation. A fixation plate was designed accordingly by defining a new surface geometry that was compatible with the humeral shaft bone and coverage of the fracture area. Additionally, flat and PPI bone plates were produced by 3D printing MJF method and their bending strength was investigated by four-point bending tests.

2. Material and Method

2.1. CAD model of left humeral bone

In the proposed methodology of this section, the humerus bone structure scanned with the CT is converted into computer-aided design (CAD) data and the plate design is prepared based on the bone model. First, to investigate the humeral bone design, the general platform of GrabCAD was used for the medical image recognition and segmentation of CT data. Then, the Geomagic (Morrisville, North Carolina, USA) software was used for optimizing the left humeral model, to create mesh geometry. Finally, the mesh model of the left humeral bone was imported to the converter surface modulus in Solidworks (Solidworks, Waltham, MA, USA). The surface model capability for shape adaptation of plate design is improved by selecting a region of interest (ROI), the area of the fracture gap expressed by the red line as seen in Figure 1a. The design of the personalized bone plates with coverage surface was as follows: the plate internal surface should be fitted with the outer surface of the humeral shaft. For this purpose, the planes that were suitable for the cross-sectional morphology were placed by slicing along the axis of the bone as illustrated in Figure 1b. Here, the distance between the slicing planes was taken as 5 mm from the reference plane, and 22 planes were acquired on the shaft and 3 planes were prepared in the part of the distal humerus close to the shaft.

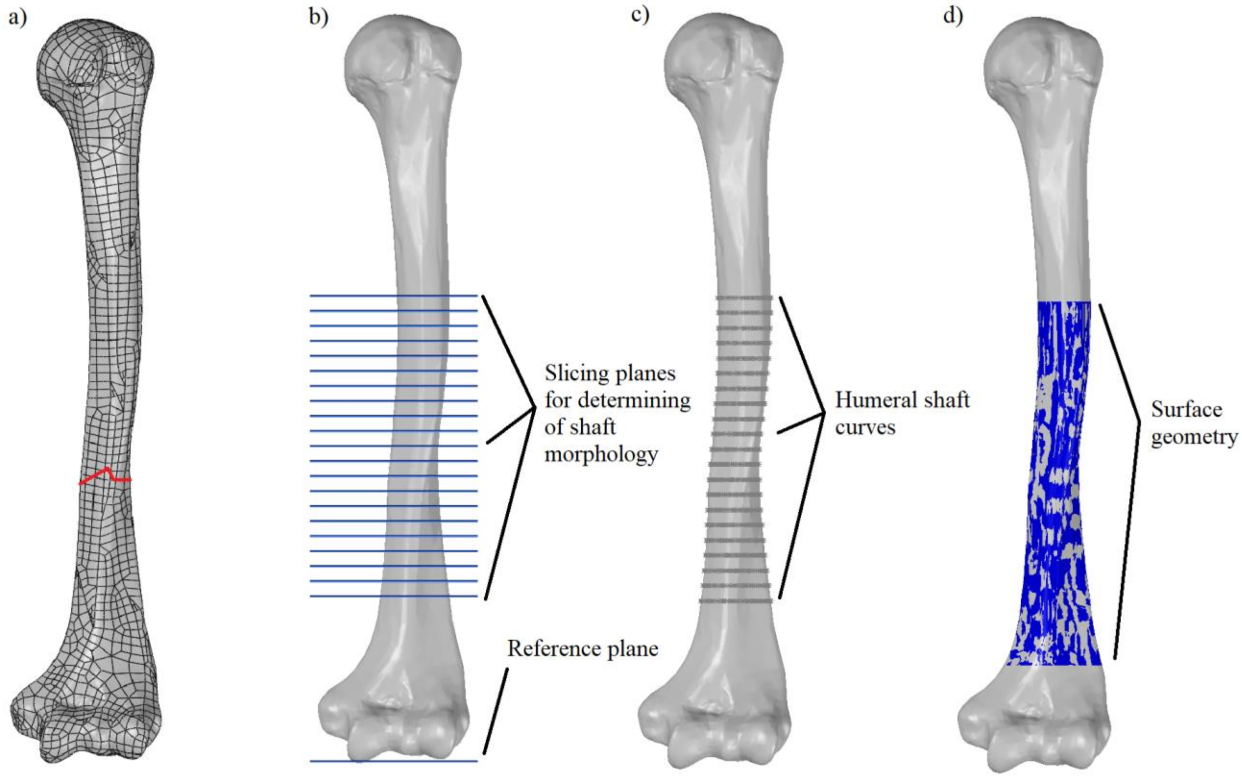

Figure 1. The solid model create from surface for bone plate design, a) Surface model, b) Slicing, c) Defining curves, d) Surface creating for ROI.

As seen in Figure 1c, the surface model was created through curves defined on the bone CAD model. Here, the surface geometry was achieved by drafting the curves which are created by a slicer for a close fit of the bone surface as given in Figure 1d. To compare the topology of the mentioned surface and mesh, deviation analysis was performed. In previous studies about geometric measurements, there was a deviation of less than 1.2 mm in whole bone geometry between the 3D model created with the MAF method (Shoulkha et al., 2011; Rashid, 2023). It is noted that by using the MAF method, wider coverage of the distal humerus part ensures that the anatomical and geometric deviation is more personalized, with an average value of 0.1-0.2 mm (Vitković et al., 2023). Eijnatten et al. (2018) determined that for the medical AM model, there was a change of 0.3-0.46 mm within the volumetric limits from CT to 3D model creation.

The volumetric model results indicated that the maximum deviation between the humerus shafts ROI and the created surface model was measured as 0.256 mm, as shown in Figure 2a. However, deviation values between ROI and the bone surface can be reduced by determining the curves of the points with maximum deviation on the humerus model.

The splines prepared on two planes with a distance of 10 and 30 mm from the reference plane were redrawn as given in Figure 2b. Then, the surface was remodeled with the new spline points and the maximum deviation value was reduced to 0.005 mm. When the deviation was controlled for the whole model including bone and humerus shafts ROI points according to the precise measurement range, the deviation values for the ROI were adjusted between 0-0.005 mm, as seen in the Figure 2c.

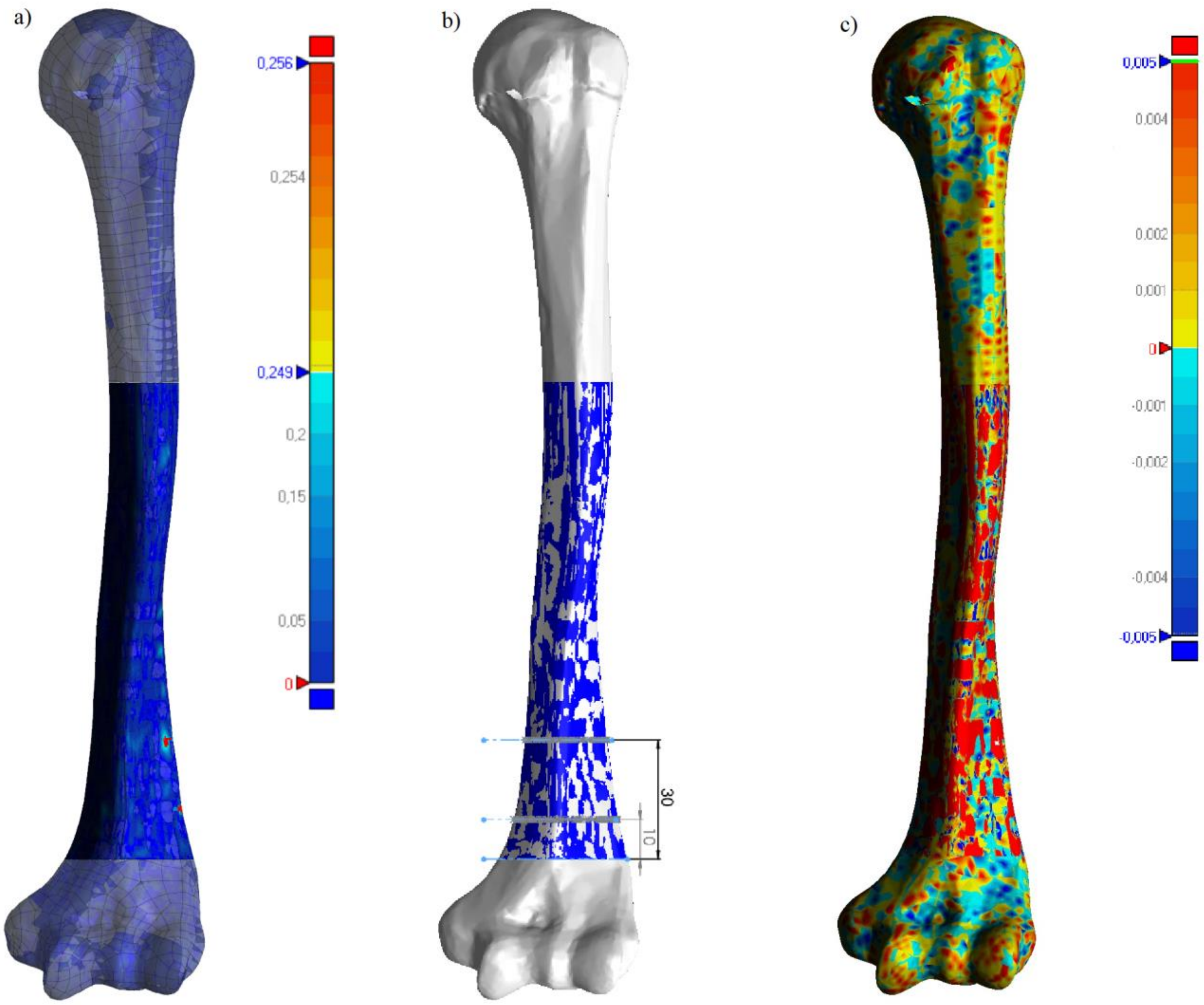

Figure 2. Improving the deviation value of the surface created on the humerus bone, a) Initial deviation, b) Determination of high deviation area, c) Homogeneous distribution of deviation value.

2.2. Preparing of fixation plate for humeral shaft

The humeral shaft plate design is classified according to humeral shaft fractures. Using the traditional plating technique, the fixation process is performed through a posterior approach. The traditional compression plate includes a radius to be compatible with the bone, as seen in Figure 3a. In the presented study, as a first approach, the humeral shaft surface where the plate is placed on the body was modeled in the previous section. In the following, a dynamic compression plate (DCP) for the left humeral shaft was generated on the bone model with adequate deviation values, as shown in Figure 3b It is noted that the surface model prepared for the new parametric model is a useful method in terms of making it possible to create a 3D plate model (Chen, 2018; Vitković et al., 2018; Vitković et al., 2023).

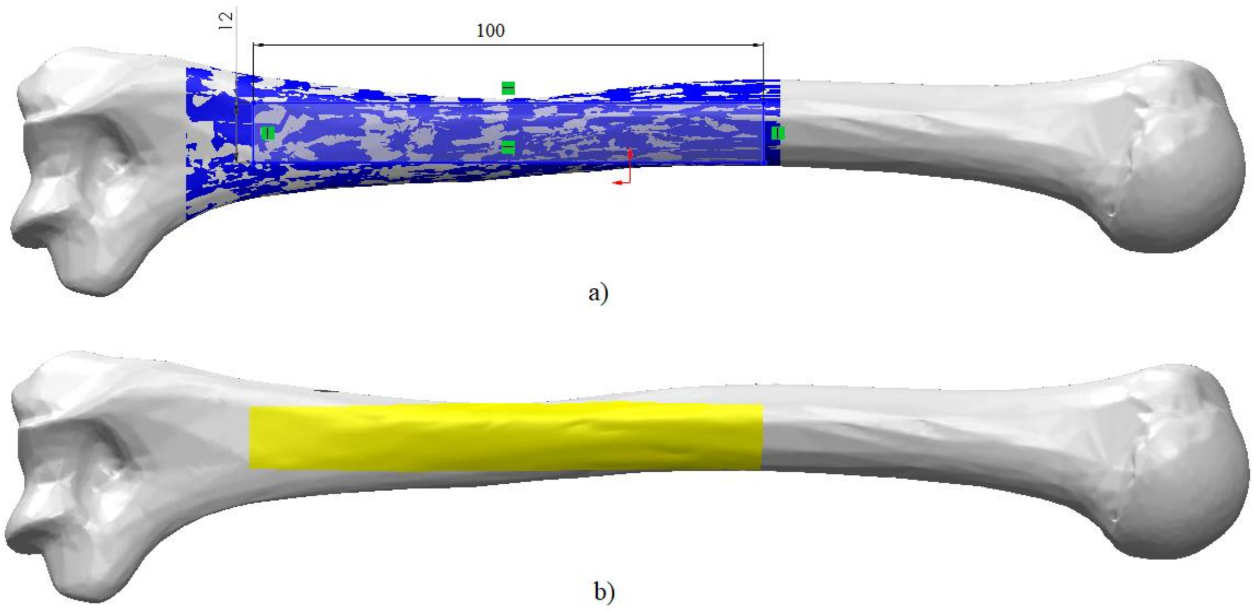

Figure 3. a) Determination of plate boundaries according to ROI region, b) Wrapping the surface according to plate dimensions.

The compression plate dimensions were 100 mm in length, 12 mm in width, and 4 mm in thickness. The screw holes were drilled on the PPI plate using a tangent plane for the 4.5 mm cortical screws. It is intended to fix the fracture area using compression plate dimensions designed for the humerus and tibia. For this purpose, a draft was used by the commands of the Solidworks software tools, and the geometry of the plate was covered on the shaft surface.

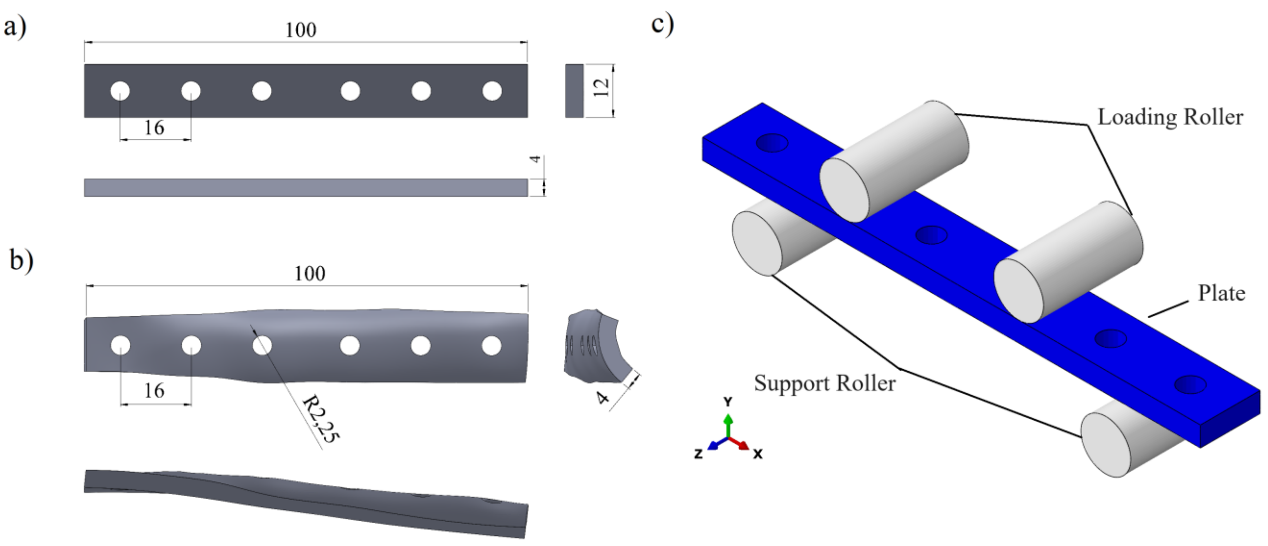

Figure 4. a) Conventional flat plate, b) PPI plate, c) FE model for four-point bending analysis.

As seen in Figure 4a and 4b the traditional flat plate and the PPI were designed with the MAF method. A scaffold covering the bone surface was obtained according to the humerus shaft topology. To ensure the compatible morphology, the Solidworks wrap command was used on the top of the plane. Then, the wrap was converted surface with 4 mm thickness. PPI design is different from the plate produced by traditional methods and fixed to the bone by the bending process during the surgical operation.

2.3. Four-point bending FE analysis of plates

To investigate the PPI and the flat plate bending stiffness, the finite element model (FEM) by Abaqus/Explicit was set up as shown in Figure 4c The bending test standards for metallic plates ASTM F382 (2018) were used in simulations to compare the bending performances of the mentioned plates. According to the ASTM F382 standard, the recommended parameters are given as follows: support roller radius of 5 mm, the distance of loading roller is 35 mm and horizontal distance between loading rollers is 22.5 mm. The plates, support, and loading roller were both meshed by hexahedral reduced integrated element (C3D8R). The loading roller was controlled by given radial displacement. The support roller was restricted rotational and axial movement for all directions. The interaction between the rollers and the outer and inner surfaces of the plates was assumed as a friction coefficient of 0.3 with tangential behavior. Focusing on rapid prototyping, the mechanical properties of carbon fiber-reinforced polyamide (PA12) were used to produce the plates from polymer-based material by the MJF method.

3. Experimental Analysis

3.1. Rapid prototyping of PPI and flat plates

To compare the four-point bending performance of the mentioned PPI and flat plates were fabricated four samples with MJF method for the smooth model as shown in Figure 5. The material was PA12, infill %100, and layer thickness 0.08 mm. A model for testing purposes was obtained using this 3D production method. The material selection is suitable for rapid prototyping but is not biocompatible for implant structure.

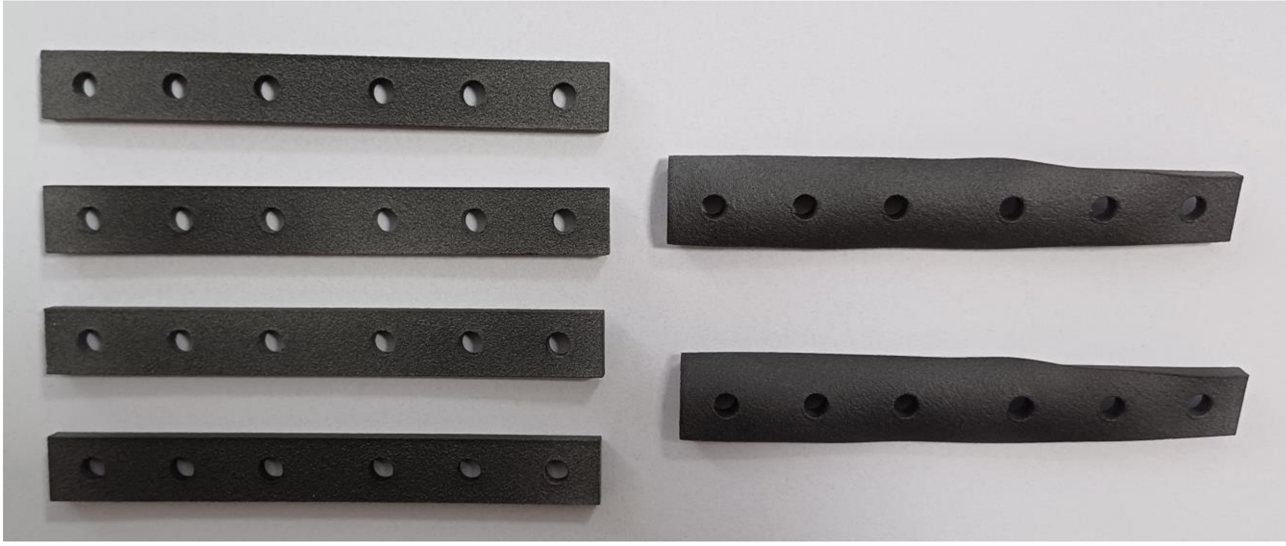

Figure 5. Flat and PPI plates produced with MJF printing method.

To evaluate the MAF design method, while adapting to the humeral bone surface, the mass of the PPI plate was greater with equal thickness, length, and width.

3.2. Tensile test of material

The material selected for the tensile test was PA12. To determine the mechanical properties of this material, four test specimens were designed according to ASTM D638-14 standard. The tensile tests were performed at a speed of 5 mm/min using a Zwick/Roell Z250 machine and 100 kN load frame. As shown in Figure 6a, the PA12 samples were assumed as isotropic and homogeneous (Erdogus, 2024).

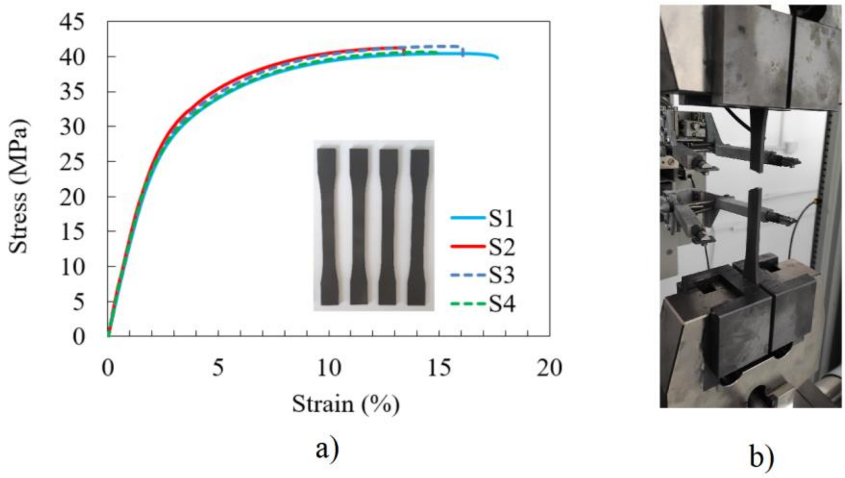

Figure 6. a) PA12 stress-strain relationship, b) Tensile tests of specimens.

3.3. Four-point bending tests

The four-point bending test of flat plates was applied as standard ASTM F382-14. To obtain the load-deformation graph, the distance between the loading rollers was set as 35 mm and the distance between the supports was set as 80 mm to prevent the plate ends from contacting the rollers during bending. As can be seen from Figure 7, tests were conducted on the flat plates using the Zwick/Roell Z250 machine, with a displacement rate of 5 mm/min**.**

Figure 7. Four-point bending tests of flat humeral bone plate.

The load-deformation curve is plotted automatically, according to this, the bending stiffness (K) was calculated from the maximum slope of this curve (ASTM F382-14). The bone plate bending structural stiffness and bending strength were calculated using the formula Eq. (1) and Eq. (2) for ASTM F382-14. Here, the proof load (P) was drawn on a line parallel to the load-deformation curve at 0.2% offset.

$$\mathrm{EI} = \frac{(2\mathrm{h} + 3\mathrm{a})\mathrm{Kh}^2}{12} \tag{1}$$

$$\text{Bending Strength} = \frac{\mathrm{Ph}}{2} \tag{2}$$

Where; h- the loading span distance, a-the center span distance, K-the bending stiffness. Le et al. (2023) designed a bone plate-like 3D-printed solid model test piece and performed a four-point bending test. Additionally, the research has been conducted on predicting mechanical behavior using machine learning.

4. Results and Discussion

The bending performances of flat and PPI plates were compared in this study. First, as given in Figure 8a, experimental results were compared according to mesh size to verify the FEM. The bone plate model was discretized by C3D8R element with mesh size 0.7 mm. To evaluate the grid size on simulation was analysed and the model was verified: the flat plate was meshed with seven layers of grids through the thickness (Figure 8b). As seen in Figure 8c, the force-deformation behavior of flat plate with experimental and numerical analysis under a four-point bending load. The tests of four flat plate samples, as given in Figure 8d, for a single cycle to determine bending stiffness, structural stiffness, and bending strength. The bending test results indicated that the maximum loads revealed no significant differences were found between test samples.

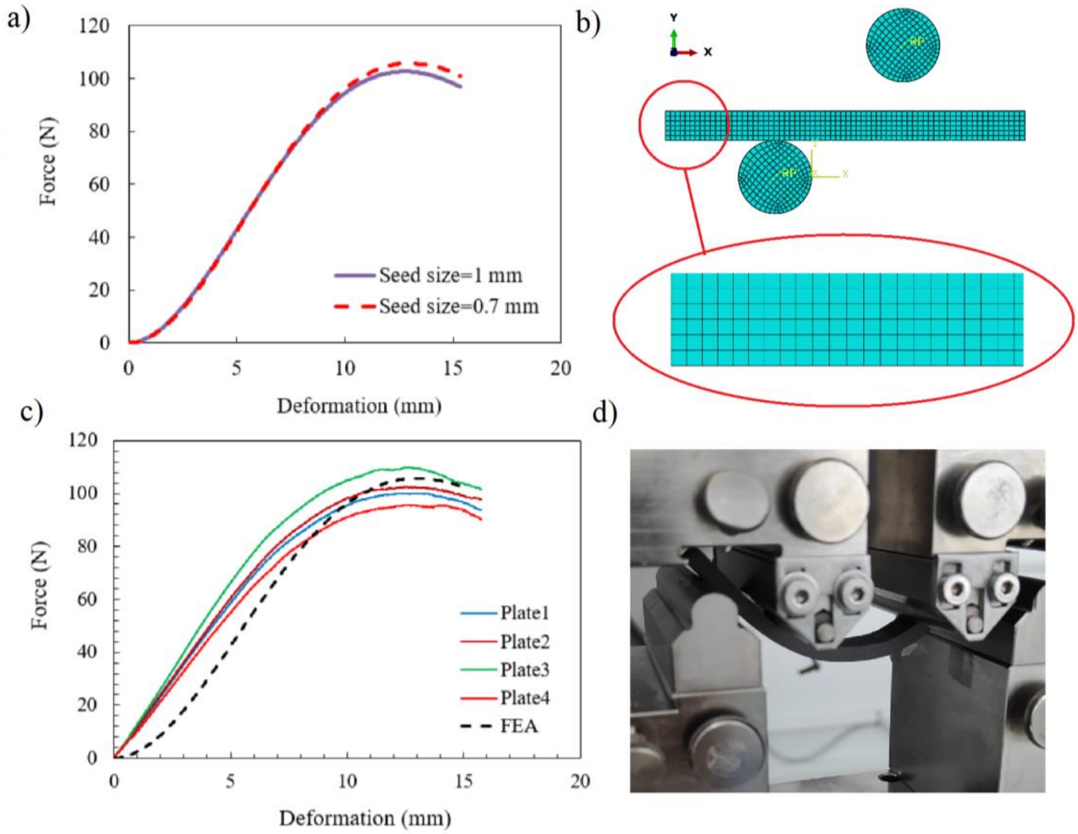

Figure 8. a) Mesh convergence according to seed size, b) Grid distribution across plate thickness, c) Comparison of force-deformation curves of flat plate, d) Experimental study.

To investigate the maximum load correlated with bending strength, the mean bending strength of the flat plate was calculated at 1148.41 ±87 N.mm, and 1188.73 N.mm was presented according to the FEA value for the force-deformation curve. In addition, the bending strength is calculated for Eq.(2) to be 2095.69 N.mm for the PPI plate for 13.36 mm radial deformation. It was observed that the same radial deformation value was 56.62% lower for a flat plate. As seen in Figure 9, the PPI plate has more resistance to bending than the flat plate. A morphology of a plate compatible with the humerus bone is advantageous in terms of bending strength compared to a flat plate by buckling inward to surround the bone. A significant difference was exhibited in the bending strength and the deformation of the plate from 0 to 15 mm between PPI and flat plate. Although it has equal length and thickness with the flat plate, its bending resistance has increased due to the increase in width according to bone morphology.

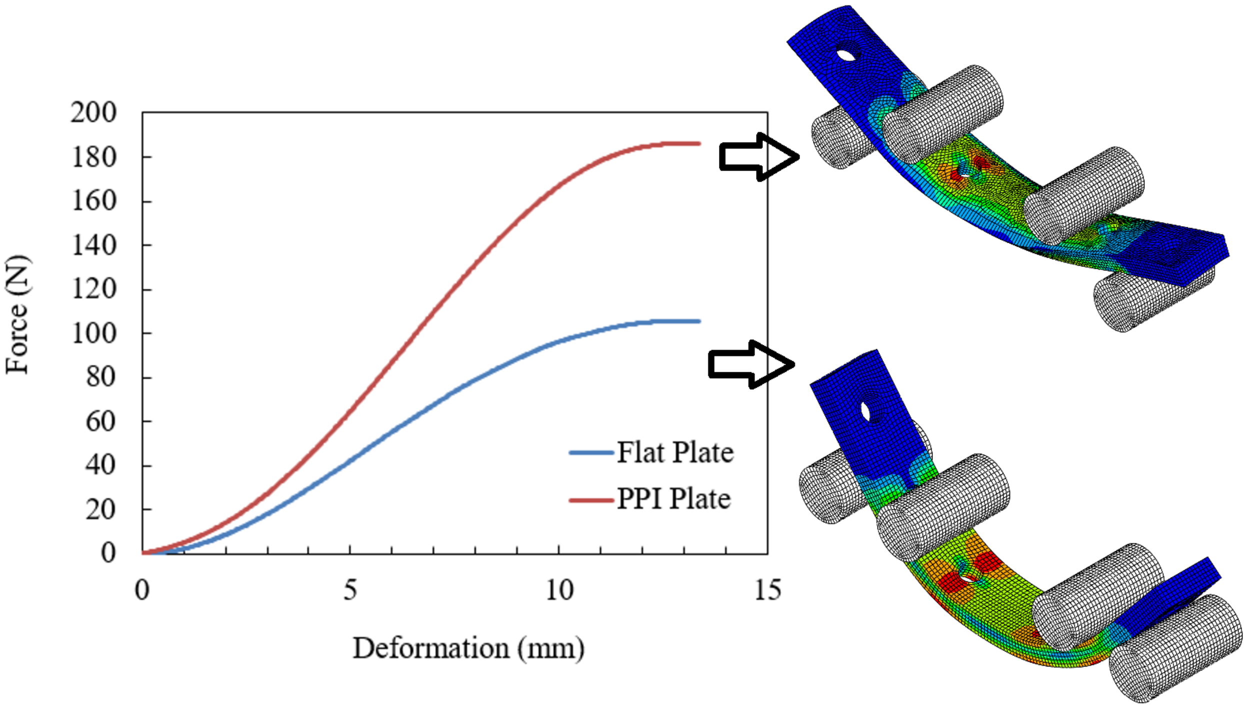

Figure 9. Comparison of different bone plate design types for force-deformation curves according to FE analysis.

An FE analysis was performed to model the bending performances of PA12 plates at an 80 mm roller span with different designs. To understand the bending resistance merits of bone plates, the construction is affected by the compatibility of the bone body. The stress shielding effect that may occur after implantation of the bone plate produced as a prototype from the same material under the same conditions was interpreted through numerical and experimental analysis. Focusing on the material selection and geometrical improvements, the stress shielding could be reduced in these results of study. In both bone plates, the stress increased on the outside of the part during bending. Here, although the two designed plates were of equal thickness, length, and width, the stress contour occurring in the PPI was less along the thickness section than in the flat plate (Figure 10).

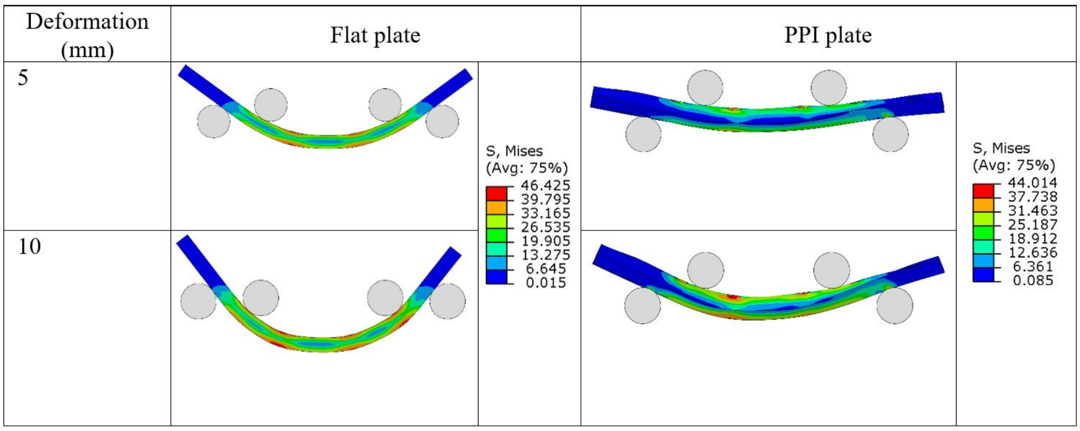

Figure 10. Stress distributions of flat and PPI plates four-point bending simulation.

The PPI plate is more resistant than flat plate because it has a variable cross-sectional area. In under bending loading, the PPI plate has an advantage due to the cross-sectional variability. It has been observed that it is more resistant to bending deformation that may occur in the fracture area of the bone. However, another important advantage of the PPI design is its adaptation to bone morphology. In addition, it is thought that the deviation between the left humerus bone and the compatible plate PPI is quite low, which provides a solution for unforeseen situations in the bone shape during the surgical operation. Since the PPI plate has a morphology compatible with humerus bone geometry, the total reaction force increased during roller displacement.

5. Conclusion

The conventional flat plates are implanted after pre-bending depending on the patient's bone tissue. In this way, an attempt is made to adapt to the individual bone geometry. In addition, bone plates with a low modulus of elasticity demonstrate higher healing performance. When preparing personalized bone plate modeling, reverse engineering and 3D printing techniques are used from a wide range of materials. In this paper, the bone plate design for a personalized approach has been presented and determined together with bending behavior. MAF was proposed in an attempt to enhance the contact surface between the plate and bone. The PPI model was created using MAF which was a reference to the left humerus bone. The results showed that the bending strength increased despite having the same geometric boundaries. Also, the results of the present study confirmed that the plate design compatible with bone morphology was stiffer in terms of bending than the flat plate. It can be expected that plate designs that are geometrically compatible with bone morphology can become more useful with mechanical tests by placing them on the bone.

Statement of Conflict of Interest

The author has declared no conflict of interest.

Author's Contributions

The contribution of the author is equal.

References

Ahmad M., Nanda R., Bajwa AS., Candal-Couto J., Green S., Hui AC. Biomechanical testing of the locking compression plate: when does the distance between bone and implant significantly reduce construct stability?. Injury 2007; 38(3): 358-364.

An Z., Zeng B., He X., Chen Q., Hu S. Plating osteosynthesis of mid-distal humeral shaft fractures: minimally invasive versus conventional open reduction technique. International Orthopaedics 2010; 34: 131-135.

Arvier JF., Barker TM., Yau YY., D'Urso PS., Atkinson RL., McDermant GR. Maxillofacial biomodelling. British Journal of Oral and Maxillofacial Surgery 1994; 32(5): 276-283.

ASTM F382-14, Standard specification and test method for metallic bone plates. ASTM International, 100 Barr Harbor Drive, PO Box C700, West Conshohocken, PA 19428-2959, United States 2014.

Chen X. Parametric design of patient-specific fixation plates for distal femur fractures. Proceedings of the Institution of Mechanical Engineers, Part H: Journal of Engineering in Medicine 2018; 232(9): 901-911.

Cousley RR., Bainbridge M., Rossouw PE. The accuracy of maxillary positioning using digital model planning and 3D printed wafers in bimaxillary orthognathic surgery. Journal of Orthodontics 2017; 44(4): 256-267.

Erdogus HB. Compression behaviour of ZPR tubular structures under axial and oblique loads. Australian Journal of Mechanical Engineering 2024; 1-14.

Huotilainen E., Paloheimo M., Salmi M., Paloheimo KS., Björkstrand R., Tuomi, J., Mäkitie A. Imaging requirements for medical applications of additive manufacturing. Acta Radiologica 2014; 55(1): 78-85.

Jabran A., Peach C., Zou Z., Ren L. Parametric design optimisation of proximal humerus plates based on finite element method. Annals of Biomedical Engineering 2019; 47: 601-614.

Jian Z., Ao R., Zhou J., Jiang X., Zhang D., Yu BA. new anatomic locking plate for the treatment of posterolateral tibial plateau fractures. BMC Musculoskeletal Disorders 2018; 19: 1-6.

Kumar C., Gupta AK., Nath R., Ahmad J. Open reduction and locking plate fixation of displaced proximal humerus fractures. Indian Journal of Orthopedics 2013; 47: 156-160.

Le C., Kolasangiani K., Nayyeri P., Bougherara H. Experimental and numerical investigation of 3D-Printed bone plates under four-point bending load utilizing machine learning techniques. Journal of the Mechanical Behavior of Biomedical Materials 2023; 143, 105885.

Liang X., Jacobs R., Hassan B., Li L., Pauwels R., Corpas L., Lambrichts I. A comparative evaluation of cone beam computed tomography (CBCT) and multi-slice CT (MSCT): Part I. On subjective image quality. European Journal of Radiology 2010a; 75(2): 265-269.

Liang X., Lambrichts I., Sun Y., Denis K., Hassan B., Li L., Jacobs R. A comparative evaluation of cone beam computed tomography (CBCT) and multi-slice CT (MSCT). Part II: On 3D model accuracy. European Journal of Radiology 210b; 75(2): 270-274.

Liao B., Sun J., Xu C., Xia R., Li W., Lu D., Jin Z. A mechanical study of personalized Ti6Al4V tibial fracture fixation plates with grooved surface by finite element analysis. Biosurface and Biotribology 2021; 7(3): 142-153.

Malik HH., Darwood AR., Shaunak S., Kulatilake P., Abdulrahman A., Mulki, O., Baskaradas A. Three-dimensional printing in surgery: a review of current surgical applications. Journal of Surgical Research 2015; 199(2): 512-522.

Majstorovic V., Trajanovic M., Vitkovic N., Stojkovic M. Reverse engineering of human bones by using the method of anatomical features. Cirp Annals 2013; 62(1): 167-170.

Marro A., Bandukwala T., Mak W. Three-dimensional printing and medical imaging: a review of the methods and applications. Current Problems in Diagnostic Radiology 2016; 45(1): 2-9.

Nowak LL., Dehghan N., McKee MD., Schemitsch EH. Plate fixation for management of humerus fractures. Injury 2018; 49: S33-S38.

Rashid MM. Anatomical personalized plate implants (APIs) are the best choice for treating distal femur fractures. Al-Qadisiyah Journal for Engineering Sciences 2023; 16(1): 30-36.

Rashid MM., Husain KN., Vitković N., Manić M., Trajanović M., Mitković MB., Mitković MM. Geometrical model creation methods for human humerus bone and modified cloverleaf plate. Journal of Scientific & Industrial Research 2017; 76: 631-639.

Rashid MM., Husain KN., Alhasoon AA. Expert system for the production of personalized cloverleaf plate implant for human humerus. In IOP Conference Series: Materials Science and Engineering 2021; 1090(1): 012099.

Ren D., Liu Y., Lu J., Xu R., Wang P. A novel design of a plate for posterolateral tibial plateau fractures through traditional anterolateral approach. Scientific Reports 2018; 8(1): 16418.

Scolaro JA., Voleti P., Makani A., Namdari S., Mirza A., Mehta S. Surgical fixation of extra-articular distal humerus fractures with a posterolateral plate through a triceps-reflecting technique. Journal of Shoulder and Elbow Surgery 2014; 23(2): 251-257.

Sholukha V., Chapman T., Salvia P., Moiseev F., Euran F., Rooze M., Jan SVS. Femur shape prediction by multiple regression based on quadric surface fitting. Journal of Biomechanics 2011; 44(4): 712-718.

Soni A., Singh B. Design and analysis of customized fixation plate for the femoral shaft. Indian Journal of Orthopaedics 2020; 54: 148-155.

Tilton M., Armstrong A., Sanville J., Chin M., Hast MW., Lewis GS., Manogharan, GP. Biomechanical testing of additive manufactured proximal humerus fracture fixation plates. Annals of Biomedical Engineering 2020; 48: 463-476.

Van Eijnatten M., van Dijk R., Dobbe J., Streekstra G., Koivisto J., Wolff J. CT image segmentation methods for bone used in medical additive manufacturing. Medical Engineering & Physics 2018: 51: 6-16.

Vitković N., Radović L., Trajanović M., Manić M. 3D point cloud model of human bio form created by applying geometric morphometrics and method of anatomical features: Human tibia example. Filomat 2019; 33(4): 1217-1225.

Vitković N., Stojković M., Majstorović V., Trajanović M., Milovanović J. Novel design approach for the creation of 3D geometrical model of personalized bone scaffold. CIRP Annals 2018; 67(1): 177-180.

Vitković N., Stojković JR., Korunović N., Teuţan E., Pleşa A., Ianoşi-Andreeva-Dimitrova A., Păcurar R. Extra-articular distal humerus plate 3D model creation by using the method of anatomical features. Materials 2023; 16(15): 5409.

Webb PA. A review of rapid prototyping (RP) techniques in the medical and biomedical sector. Journal of Medical Engineering & Technology 2000; 24(4): 149-153.